

Charge Dynamics in Electron-Irradiated Polymers*

G. M. Sessler and G. M. Yang

University of Technology, D-64283 Darmstadt, Germany

Received 23 June, 1998

Recent studies of charge trapping and charge transport in polymer films irradiated and charged with monoenergetic electrons of range smaller than the sample thickness and thereafter stored or annealed under various conditions are discussed. An analytical model used to describe the phenomena takes the following parameters into consideration: Charge and energy deposition profiles, charge drift due to a shallow-trap-modulated mobility, deep trapping without release, trap filling due to a finite trap density, and ohmic relaxation due to a radiation-induced conductivity during irradiation and its delayed component after irradiation. The model calculations show the effect of various parameters on the shape of the initial charge distribution and on its evolution with annealing time. - Experiments with the laser-induced pressure-pulse (LIPP) method on 12 and 25 μm thick fluorocarbon and polyimide films, charged with 10 or 20 keV electron beams, respectively, yield the charge distributions after irradiation and the changes of the distributions due to annealing of the samples at 120°C for various times. A comparison of experimental and analytical results reveals the trapping kinetics and permits to estimate the deep-trap density and the $\mu\tau$ -product, where μ is the trap-modulated mobility and τ is the trapping time.

I Introduction

The understanding of charge trapping and charge transport in electron-irradiated polymers has greatly benefited from the work of Bernhard Gross. In particular, his investigations of the effects of ionizing radiation on such phenomena as charge buildup [1], charge dynamics [2,3], radiation-induced conductivity [4,5], space-charge limited currents [6], and electron transmission [7] are milestones in this field. The insights gained from these studies have been the foundation for much of the work on charging phenomena in irradiated dielectrics during the last two or three decades.

Interest in electron-irradiated dielectrics, particularly polymers, was at least in part due to space applications of these materials, for example as thermal blankets for spacecraft, which are exposed to low-energy electrons. Apart from this, electron irradiation experiments allow one to study charge dynamics in the bulk of insulators under conditions where surface effects can often be neglected [8].

The work of Gross on charge dynamics in irradiated dielectrics made it particularly desirable to study, with relatively high resolution, the charge distributions in such substances. Appropriate experimental methods, based on acoustic or thermal excitation of the samples,

were developed over the past 10 to 15 years and are now capable of a resolution of about 1 μm . Such measurements have resulted in a vast amount of data on charge distributions and charge dynamics in thin polymer films and other dielectrics [9]-[11] (and references therein).

In the present paper, charge trapping and charge transport in 12 and 25 μm thick fluorocarbon (FEP) and polyimide (PI) films, charged at room temperature with monoenergetic electron beams and annealed thereafter, is studied both numerically and experimentally. The results yield information about charge-transport processes in these polymers.

II Simulation of charge transport

II.a Model for charging

Corresponding to the experimental procedure, a two-stage process of charge transport is assumed, consisting of a room-temperature charging period and an elevated-temperature annealing period, as shown in Fig. 1.

Thus, the dielectric is electron-beam charged at room temperature from time $t = 0$ to $t = t_b$. Dur-

*Dedicated to Prof. Dr. Bernhard Gross

ing this time, there is considerable charge rearrangement due to drift and radiation-induced conductivity (RIC); in addition, there is some deep trapping. Following this period, the dielectric is stored from $t = t_b$ to $t = t_0$ at room temperature to allow for some more charge motion due to drift and the delayed component of the RIC [2, 5] and eventual deep trapping of all charges. Thereafter, the sample is quickly heated to an elevated temperature (120°C in the experiment) where there is complete detrapping and drift of the charges in their own field until they are deeply trapped again. As seen in Fig. 1, the sample is kept at the annealing temperature for a time period t_a ; thereafter, its charge distribution is determined.

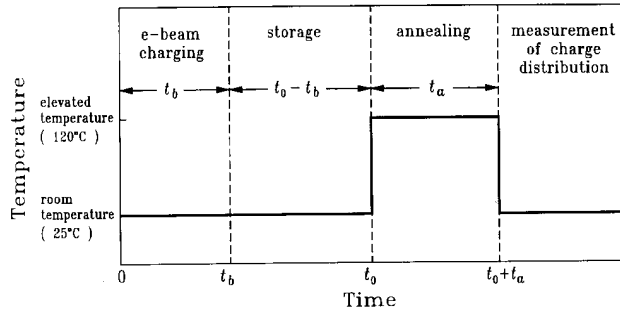


Figure 1. Temperature cycle and time scales of the experiments.

The charging process, depicted in Fig. 2, and the room-temperature storage can be described by the equation of continuity, the Poisson equation, and the rate equation. These are respectively given by

$$\epsilon \frac{\partial E(x, t)}{\partial t} + [\mu \rho_f(x, t) + g(x, t)] E(x, t) + I(x) = I_0, \quad (1)$$

$$\epsilon \frac{\partial E(x, t)}{\partial x} = \rho(x, t), \quad (2)$$

$$\frac{\partial \rho_t(x, t)}{\partial t} = \frac{\rho_f(x, t)}{\tau} \left[1 - \frac{\rho_t(x, t)}{\rho_m} \right]. \quad (3)$$

In these equations, $E(x, t)$ is the electric field, I_0 and $I(x)$ are the current densities of the incident electron beam and the electron beam at depth x in the dielectric, respectively, $\rho_f(x, t)$ and $\rho_t(x, t)$ are the charge densities of mobile and trapped charges, respectively, $\rho(x, t)$ equals $\rho_f(x, t) + \rho_t(x, t)$, μ is the shallow-trap-modulated mobility of the mobile charges, $g(x, t)$ and

ϵ are the RIC and the dielectric permittivity, respectively, and τ is the trapping time. In the rate equation (3) it is assumed that the electrons are captured in deep traps of density ρ_m and no release is possible. The use of Eqs. (1) to (3) for analyzing the charging process and the proper choice of parameters, including the radiation-induced conductivity, have been discussed in detail in [10].

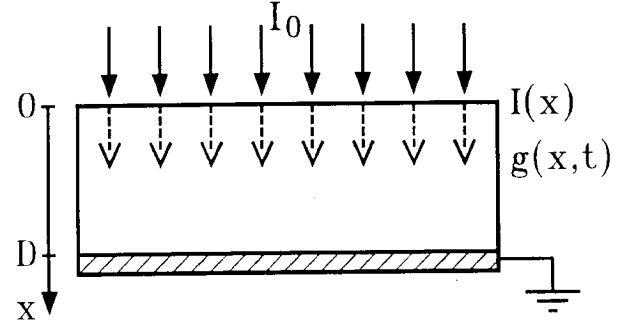


Figure 2. Open-circuit electron-beam charging of dielectric.

II.b Model for annealing

In the case of *fast retrapping* during annealing, as encountered in FEP at 120°C (see below), charge transport can also be explained with Eqs. (1) to (3) by setting I_0 and $I(x)$ equal to zero. Now, the charge trapped in the dielectric at room temperature is assumed to be detrapped at the elevated temperature and to undergo drift and a second deep-trapping process with values of the constants ϵ , μ , g , τ , and ρ_m possibly different from those prevailing at room temperature, as discussed in Sect. II.c.

For *slow retrapping* during annealing, as found in PI at 120°C (see below), a very simple model assuming gradual release of the trapped charges at the elevated temperature and subsequent drift to the sample electrode may be used. Since the number of released charges is proportional to the charge density $\rho(x, t)$, and the released charges remain in the sample for a negligible time, one has after the annealing time t_a

$$\rho(x, t) = \rho(x, t_0) e^{-t_a/\tau'} \quad \text{for } t \geq t_0 + t_a. \quad (4)$$

where τ' is a time constant characteristic for charge release. The same relation holds if charge compensation by holes injected through the electrode takes place.

II.c Results of model calculations

The charge distribution at $t = t_0$ is obtained by numerical evaluation of Eqs. (1) to (3) for the following parameters: Electron-beam current density $I_0 = 2 \text{ nA/cm}^2$, $t_b = 50 \text{ s}$, $t_0 = 700 \text{ s}$, in all cases and electron-beam voltage 10 keV , $\mu\tau = 2 \times 10^{-11} \text{ cm}^2/\text{V}$, $\rho_m = 0.004 \text{ C/cm}^3$ for FEP and electron-beam voltage 20 keV , $\mu\tau = 2 \times 10^{-10} \text{ cm}^2/\text{V}$, $\rho_m = 0.008 \text{ C/cm}^3$ for PI, respectively. The $\mu\tau$ -values are assumed to be valid at room temperature. Other quantities used in these calculations are given in [10].

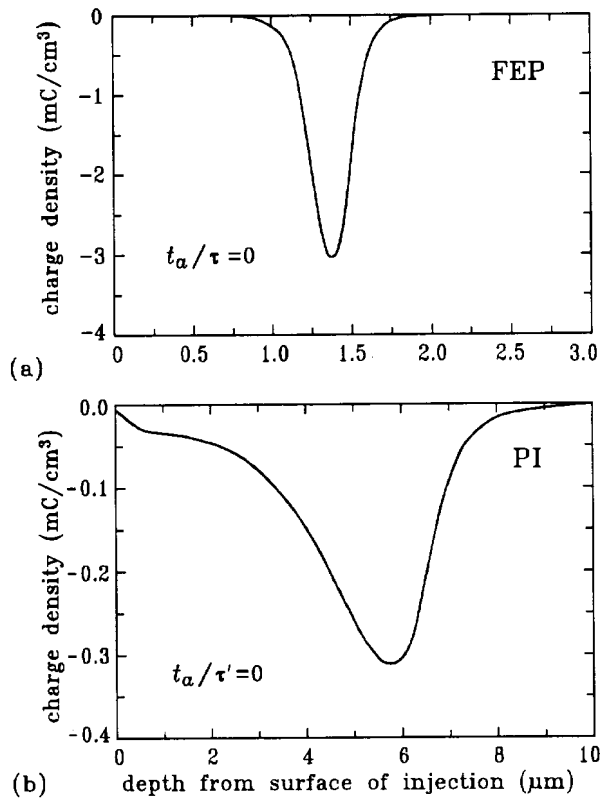


Figure 3. Distribution of total charge ρ (equal to trapped charge ρ_t) at $t_0 = 700 \text{ s}$ in FEP (part a) and PI (part b) after room temperature charging. Electron injection at depth $0 \mu\text{m}$, electrode at $12 \mu\text{m}$ (FEP) or $25 \mu\text{m}$ (PI).

The distributions so obtained are depicted in Figs. 3a and 3b. They consist only of deeply-trapped charges, such that $\rho = \rho_t$, since after the (long) time t_0 all the originally mobile carriers are deeply trapped. For the $\mu\tau$ -values used, the shape of the distributions is mainly determined by the RIC and its delayed component and to a lesser extent by mobility. The distributions are therefore more or less limited to the irradiated volume of the samples [10]. These distributions are used as

the initial data for the simulation of charge transport during the annealing period.

For *fast retrapping* (FEP) the evolution of $\rho(x, t)$ during annealing is again calculated with Eqs. (1) to (3), as discussed above. In using these equations for describing charge dynamics at the annealing temperature, the distribution shown in Fig. 3a is used as the initial distribution and appropriate values of ϵ , μ , g , τ , and ρ_m are substituted as follows.

While the dielectric permittivity of FEP remains at 2.1 between 20 and 120°C , the delayed RIC decays by about two orders of magnitude during the storage time $t_0 - t_b$ and can therefore be neglected during the annealing cycle. The deep-trap density is not expected to be temperature dependent, thus the above value of ρ_m is used. However, the temperature dependence of μ and τ has to be considered. Since the solutions depend mainly on the $\mu\tau$ -product, this parameter is adjusted for best fit with the experimental results.

Charge distributions so obtained are shown in Figs. 4 and 5. They were calculated with the values $\mu\tau = 5 \times 10^{-10} \text{ cm}^2/\text{V}$ and $\mu\tau = 10^{-9} \text{ cm}^2/\text{V}$, respectively. Parameter in these figures is the normalized annealing time t_a/τ . As seen from these plots, the deeply-trapped charge is accumulating near the location of the initial charge, while the mobile charge has a peak near the progressing charge front in the nonirradiated volume. Of interest for comparison with experimental results is the total charge $\rho(x, t)$, i. e. the sum of trapped and mobile charge.

For *slow retrapping* (PI), the evolution of the charge distribution, as obtained from Eq. (4) with $\rho(x, t_0)$ given by Fig. 3b, is depicted in Fig. 6 for different values of t_a/τ' . The decay is due to detrapping, as discussed above. The shape of the distribution is preserved, only its amplitude changes.

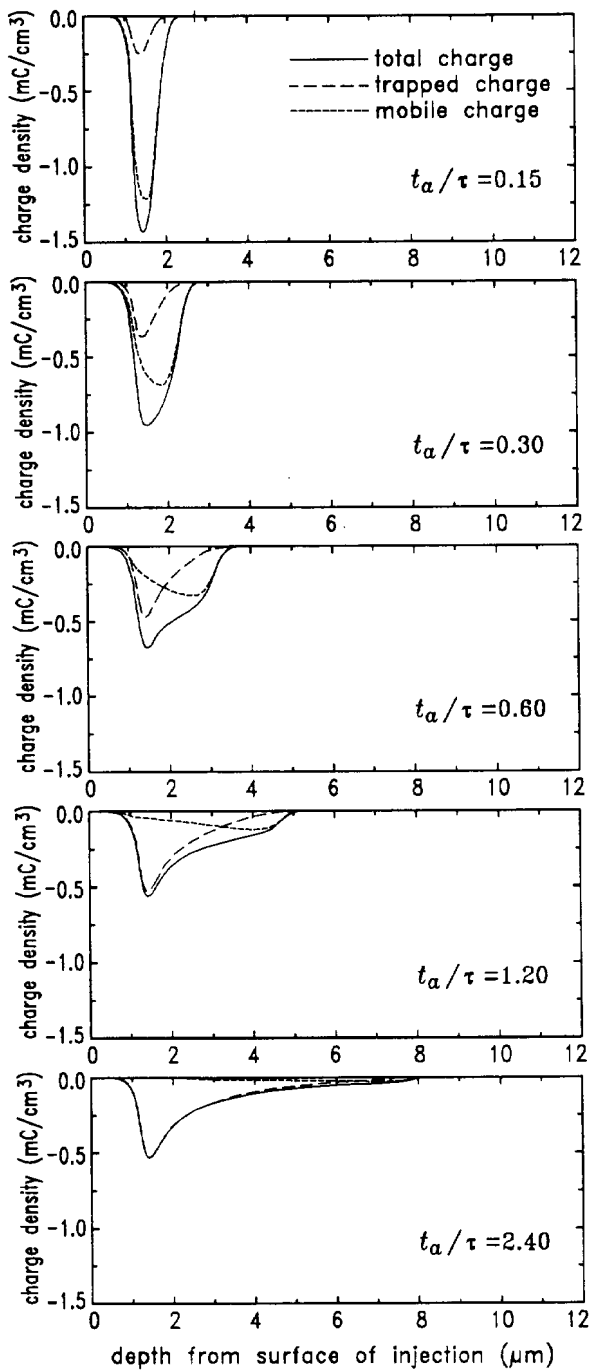


Figure 4. Evolution of total charge ρ , deeply-trapped charge ρ_t , and mobile charge ρ_f during annealing under fast retrapping conditions: Results of model calculation for $\mu\tau = 5 \times 10^{-10} \text{ cm}^2/V$.

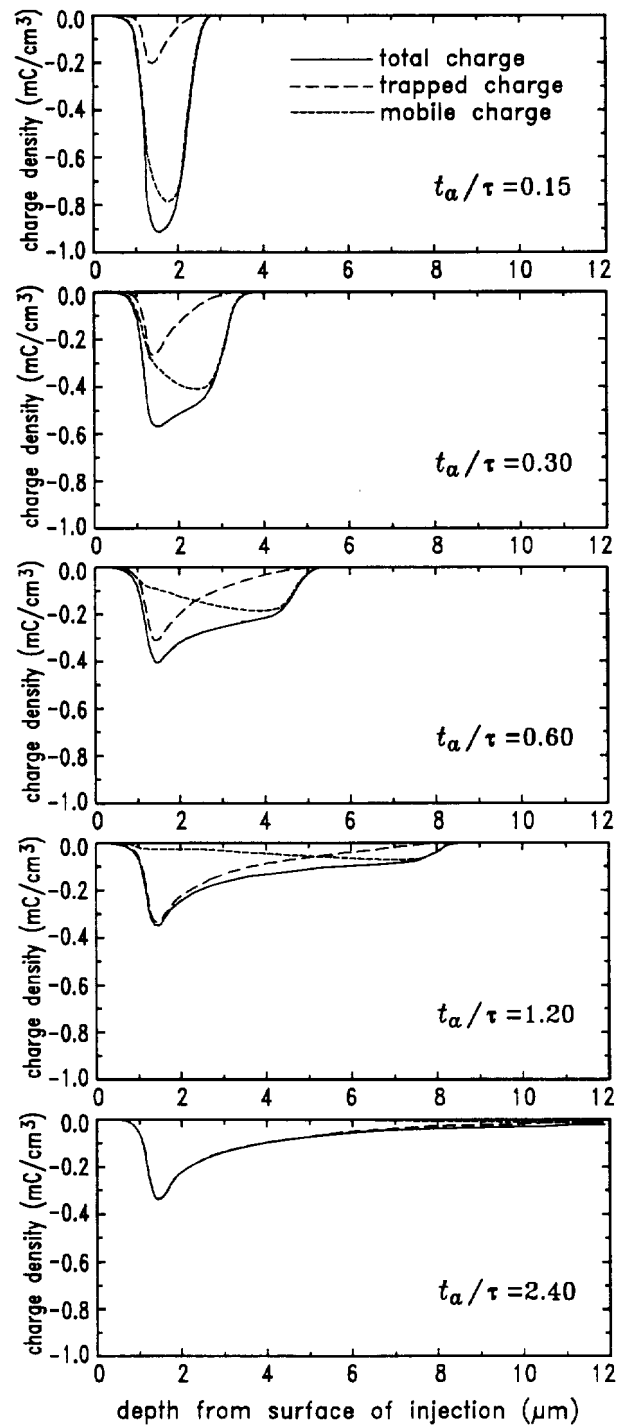


Figure 5. Evolution of total charge ρ , deeply-trapped charge ρ_t , and mobile charge ρ_f during annealing under fast retrapping conditions: Results of model calculation for $\mu\tau = 10^{-9} \text{ cm}^2/V$.

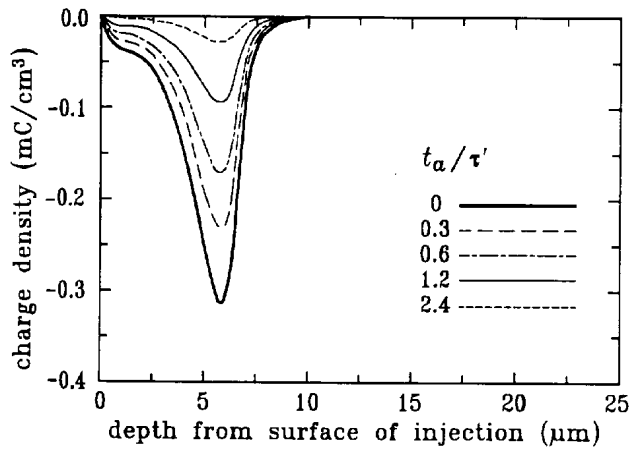


Figure 6. Evolution of total charge ρ during annealing under slow retrapping conditions: Results of model calculation.

III Experimental results

Teflon (FEP) samples of $12 \mu\text{m}$ thickness and Kapton (PI) samples of $25 \mu\text{m}$ thickness, metalized with aluminum on one side, are charged in vacuum through their nonmetalized surface with 10 keV or 20 keV monoenergetic electron beams, respectively, of current density 2 nA/cm^2 to a charge density of 100 nC/cm^2 . Following the charging process, the samples are removed from vacuum. After room-temperature storage (typically about 10 minutes), the samples are annealed at 120°C for time periods of a few minutes to a few hours. During charging and annealing, the samples are, due to the absence of a front electrode, in open circuit.

The laser-induced pressure-pulse (LIPP) method is used to measure the charge distribution in the samples. In these experiments, short (70 ps) and energetic (1 to 10 mJ) laser pulses from a mode-locked Nd:YAG laser are absorbed in a graphite layer deposited onto the sample electrode. The resulting stress effects generate a pressure pulse. This pulse propagates through the sample with the velocity of sound c and generates a current $I(t)$ in the measuring circuit which is proportional to the charge density at depth $x = ct$ in the dielectric. Details of the LIPP method are given in [12, 13].

A typical LIPP-response for FEP is shown in Fig. 7. It consists of a negative peak E due to the injected electron charge as well as positive peaks R and F caused by the induction charge on the electrode and by a positive surface charge due to secondary emission, respectively.

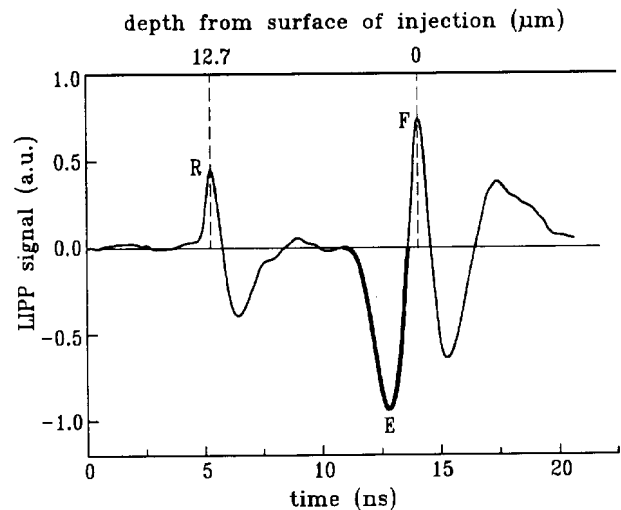


Figure 7. LIPP response for FEP, charged with 10 keV electron beam, directly after charging. Electron injection through the nonmetalized front side F of the sample. Charge layer at E . Laser pulse absorbed at rear electrode R , where the laser-induced pressure pulse is generated.

From such responses, obtained for different annealing periods, the sections containing the space-charge peak (part E of the response, depicted as a heavy line) are extracted and plotted in Fig. 8. Note the opposite direction of the depth scale in Figs. 7 and 8, necessitated by the fact that electron injection and LIPP generation occur on opposite sample surfaces.

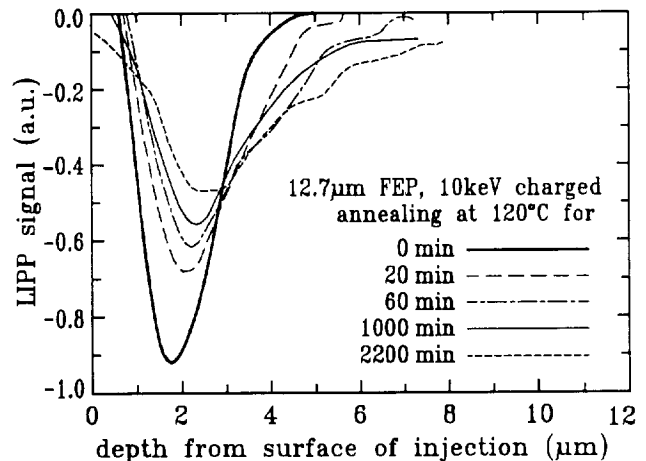


Figure 8. Change of the charge distribution in FEP sample after different annealing periods. Sample originally charged with 10 keV electron beam through front side at $0 \mu\text{m}$. Electrode at $12.7 \mu\text{m}$.

Figure 8 shows the evolution of the space charge under 120°C annealing. The results in Fig. 8 have been normalized by means of measurements of the surface potential of the samples, as shown in Fig. 9. Such a normalization is necessary since the amplitude of the LIPP

responses depends on the energy of the laser pulses which varies somewhat from pulse to pulse.

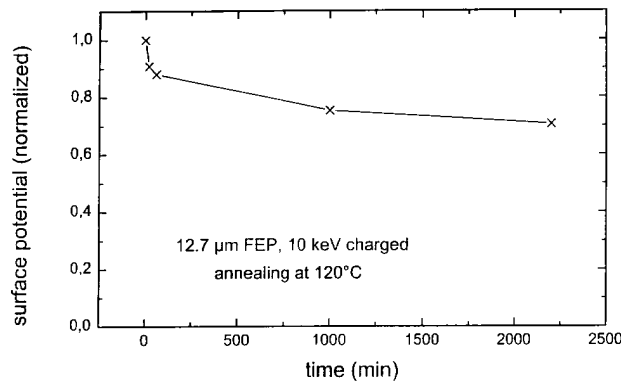


Figure 9. Decay of surface potential of Teflon FEP as function of annealing time at 120°C . Sample originally charged with 10 keV electron beam.

Figure 8 indicates that in FEP the charge motion at 120°C results in a broadening of the charge peak. The broadening is in the direction toward the electrode. This fact, together with the observation that the surface potential decays only slightly ($\sim 30\%$ for 2000 min annealing) strongly suggests that the charge decay is caused by fast retrapping of the electrons activated from the original charge layer. Similar conclusions have been reached for negative charge transport in FEP before [14]-[17]. However, a detailed picture of the evolution of the charge distribution, as seen in Fig. 8, had not been obtained yet. The Schubweg is estimated from Fig. 8 to be about $5\ \mu\text{m}$ or less (see Sect. IV).

The “smearing-out” of the charge layer toward the electrode is responsible for most of the observed surface potential decay shown in Fig. 9. It is possible that a small part of the decay is due to hole drift to the charge layer; however, this process is believed to be minor since it would not result in a broadening of the negative charge layer. Instead it would, in the absence of hole injection through the electrode [18], cause a negative depletion layer in the entire region between electrode and charge layer, which is not observed. Thus, the predominant transport process in FEP consists in activation and fast retrapping of the originally-deposited charges.

The experimental results for PI are shown in Fig. 10. The figure indicates that there is no charge accumulation between the original charge layer and the electrode as the charge decays. The charge peak, although chang-

ing its amplitude, does not broaden or smear out. On the contrary, it appears to narrow down during annealing. Thus, the charge decay must be caused by one of the following processes: (1) Detrapping of the electron-beam deposited charge and drift in the internal field to the electrode without deep retrapping, or (2) compensation of the electron-beam deposited charge by holes either injected through the electrode and drifting in the internal field without deep trapping or coming from the free surface which is positively charged due to secondary emission. The fact that the layer narrows with annealing time indicates that the second mechanism is at least partially responsible for the decay. In both cases, the charge drift is characterized by slow retrapping with electron or hole Schubwegs of about $20\ \mu\text{m}$ or more. Compensation of the original charge by *intrinsic* holes is ruled out since this process would result in a negative space charge in the region which supplies the holes. A similar compensation of electron-beam deposited charges in PI by positive carriers, resulting also in a narrowing of the charge distribution, was even observed at room temperature [19].

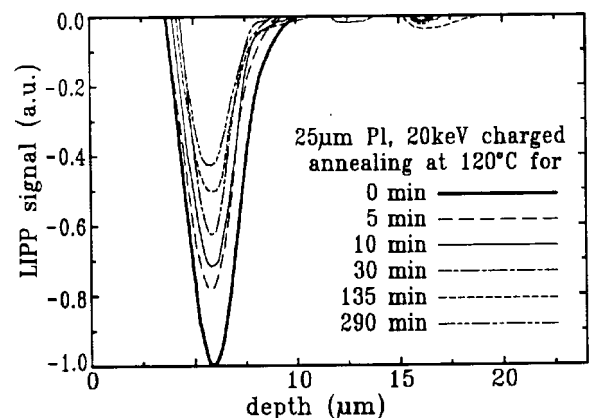


Figure 10. Change of the charge distribution in PI sample after different annealing periods. Sample originally charged with 20 keV electron beam through front side at $0\ \mu\text{m}$. Electrode at $2/5\ \mu\text{m}$.

IV Comparison with model calculations and discussion

Comparison of the experimental results for FEP in Fig. 8 with the theoretical results in Figs. 4 and 5 shows that the relatively simple model of charge transport describes the observed charge distributions reasonably

well if $\mu\tau$ at 120°C is chosen in the region of 0.5 to $1 \times 10^{-9} \text{ cm}^2/\text{V}$ with $\tau \approx 100$ min. For these values, a Schubweg of $s = \mu\tau E$ of 2.5 to $5 \mu\text{m}$ is expected for $E = 0.5 \times 10^6 \text{ V/cm}$ (this E-value corresponds to the injected charge density of 10^{-7} C/cm^2). A Schubweg of a few μm is consistent with the results in Fig. 8. The original location of the charge peak is at $1.7 \mu\text{m}$, as compared to the predicted location at $1.4 \mu\text{m}$, and the observed and calculated final distributions extend beyond $8 \mu\text{m}$.

For very large annealing times of the FEP samples, the assumption of deep trapping without release should be somewhat modified. Eventual detrapping and retrapping of the deeply trapped charge explains the slight decrease in peak amplitude and the slow "motion" of the peak toward the electrode observed at annealing times of 1000 and 2200 min and not expected from the theoretical results in Figs. 4 and 5.

The value of $\mu\tau$ used above may be compared with elevated-temperature results obtained by other authors for FEP. TSC measurements at 150°C to 200°C yielded values of about $10^{-9} \text{ cm}^2/\text{V}$ [20,21] while isothermal charge-decay experiments at 145°C gave $6 \times 10^{-9} \text{ cm}^2/\text{V}$ [14]. The $\mu\tau$ -value following from the present evaluation is thus in reasonable agreement with older data.

For PI, the experimental results in Fig. 10 also compare favorably with the analytical data in Fig. 6. In particular, the measured and calculated peak locations are both at $5.7 \mu\text{m}$ and the observed charge penetration of about $10 \mu\text{m}$ is well reproduced by theory. The major difference is the absence of negative charge close to the free surface in the experimental data. This may be due to compensation by positive surface charges generated by secondary emission during charging. These positive charges are not considered in the model calculations. The contraction of the charge layer appears to be due to charge compensation by holes, as discussed above, which is also not included in the model.

Since the charge carriers are subject to slow retrapping in PI at 120°C , the $\mu\tau$ -product at this temperature can not be determined; however, a lower limit of $6 \times 10^{-9} \text{ cm}^2/\text{V}$ follows from an estimate of the minimum Schubweg ($20 \mu\text{m}$, see above) and the electric field in the sample. To the knowledge of the authors, no $\mu\tau$ -data for this material is available in the literature for

temperatures around 120°C .

The application of analytical models to measured distribution data is a potentially powerful method for finding the mechanisms underlying charge transport in polymers. The present study is only a first step in this direction. More refined models taking into consideration other phenomena affecting carrier drift and additional measurements will lead to a better understanding of charge transport in disordered systems.

Acknowledgment

The authors are grateful to Dr. Tilman Motz for maintaining the laser and electron-beam systems used in the experiments.

References

- [1] B. Gross, J. Dow, and S. V. Nablo, "Charge buildup in electron-irradiated dielectrics", *J. Appl. Phys.* **44**, 2459-2463 (1973).
- [2] B. Gross, G. M. Sessler, and J. E. West, "Charge dynamics in electron-irradiated polymer-foil electrets", *J. Appl. Phys.* **45**, 2841-2851 (1974).
- [3] B. Gross, and G. F. Leal Ferreira, "Analytic solution for radiation-induced charging and discharging of dielectrics", *J. Appl. Phys.* **50**, 1506-1511 (1979).
- [4] B. Gross, H. von Seggern, and D. A. Berkley, "Long term behavior of radiation-induced currents in fluorinated ethylene propylene copolymer", *phys. stat. sol. (a)* **79**, 607-615 (1983).
- [5] B. Gross, R. M. Faria, and G. F. Leal Ferreira, "Radiation-induced conductivity in Teflon irradiated by x rays", *J. Appl. Phys.* **52**, 571-577 (1981).
- [6] B. Gross and L. Nunes de Oliveira, "Transport of excess charge in electron-irradiated dielectrics", *J. Appl. Phys.* **45**, 4724-4729 (1975).
- [7] B. Gross, R. Gerhard-Multhaupt, K. Labonte, and A. Berraissoul, "Current transmission and charge deposition in polyethyleneterephthalate (PETP) irradiated with 10 - 50 keV electrons", *Colloid and Polymer Sci.* **262**, 93-98 (1984).
- [8] B. Gross, "Radiation-Induced Charge Storage and Polarization Effects", in "Electrets" (G. M. Sessler, Ed.), 2nd Edition 1987, pp. 217-284.
- [9] G. M. Sessler, "Charge Distribution and Transport in Polymers", *IEEE Trans. Diel. and Electric. Insulat.* **4**, 614 - 628 (1997).
- [10] G. M. Sessler, "Charge Dynamics in Irradiated Polymers", *IEEE Trans. Electric. Insulat.* **27**, 961-973 (1992).

- [11] G. M. Yang and G. M. Sessler, "Charge Distributions in Electron-Beam Irradiated Kapton PI and Teflon FEP Films", *Proceed. 8th Internat. Sympos. Electrets* (IEEE, Piscataway, N.J., 1994), 248-253.
- [12] G. M. Sessler, J. E. West, R. Gerhard-Multhaupt, and H. von Seggern, "Nondestructive Laser Method for Measuring Charge Profiles in Irradiated Polymer Films", *IEEE Trans. Nucl. Sci.* **NS-29**, 1644-1649 (1982).
- [13] R. Gerhard-Multhaupt, "Analysis of Pressure-Wave Methods for the Nondestructive Determination of Spatial Charge or Field Distributions in Dielectrics", *Phys. Rev. B*, **27**, 2494-2503 (1983).
- [14] H. von Seggern, "A New Model of Isothermal Charge Transport for Negatively Corona-Charged Teflon", *J. Appl Phys.* **50**, 7039-7043 (1979).
- [15] C. Alquié, F. Chapeau, and J. Lewiner "Evolution of Charge Distributions in F.E.P.-Films Analysed by the Laser Induced Acoustic Pulse Method" in 1984 Annual Report, Conference on Electrical Insulation and Dielectric Phenomena (IEEE, 1984), pp. 488-494.
- [16] R. Gerhard-Multhaupt, W. Künstler, G. Eberle, W. Eisenmenger, and G. Yang, "High space-charge densities in the bulk of fluoropolymer electrets detected with piezoelectrically generated pressure steps" in *Space Charge in Solid Dielectrics*; Edited by J. C. Fothergill and L. A. Dissado (The Dielectrics Society, 1998) pp. 123-132.
- [17] O. N. Oliveira and G. F. Leal Ferreira, "Electron Transport in Corona Charged 12 μm Teflon FEP with Saturable Deep Traps", *Appl. Phys.* **A42**, 213 (1987).
- [18] G. F. Leal Ferreira and M. T. Figueiredo, "Corona Charging of Electrets", *IEEE Trans. Electric. Insulat.* **27**, 719 (1992).
- [19] M.-P. Cals, J.-P. Marque, and C. Alquié, "Direct Observation of Space Charge Evolution in e-irradiated Kapton Films", *IEEE Trans. Electric. Insulat.* **27**, 763 (1992).
- [20] R. A. Creswell, M. M. Perlman, and M. A. Kabayama, "The Electret Properties of a Series of Corona-Charged Substituted Polyolefins", in *Dielectric Properties of Polymers*, (Plenum, New York, 1972), 295-312.
- [21] H. von Seggern, "Thermally Stimulated Decay of Negatively Charged Teflon-FEP" in 1980 Annual Report, Conference on Electrical Insulation and Dielectric Phenomena (IEEE 1980), pp. 345-352.